

# CP/MAS $^{13}\text{C}$ NMR Spectra of Frozen Solutions of Poly(vinyl alcohol) with Different Tacticities

Fumitaka Horii,\* Kenji Masuda, and Hironori Kaji

Institute for Chemical Research, Kyoto University,  
Uji, Kyoto 611, Japan

Received November 19, 1996

Revised Manuscript Received February 5, 1997

It is known that the  $^{13}\text{C}$  resonance line of CH carbons of poly(vinyl alcohol) (PVA), which are obtained by CP/MAS  $^{13}\text{C}$  NMR spectroscopy, splits into three lines (lines I, II, and III) in the solid state (see Figure 1c).<sup>1–3</sup> This split is mostly thought to be due to the formation of two, one, and no intramolecular hydrogen bond(s) in the triad sequences  $[\text{CH}(\text{OH})-\text{CH}_2-\text{CH}(\text{OH})-\text{CH}_2-\text{CH}(\text{OH})]$ , but another interpretation in terms of the substitution effects of OH groups is proposed from the experimental and theoretical sides.<sup>4,5</sup> We have recently confirmed the previous assignment based on the formation of intramolecular hydrogen bonding by clarifying that the relative integrated intensities of lines I, II, and III significantly depend on casting solvents, annealing, drawing, and ambient temperature even for PVA samples with the same tacticities.<sup>2,3,6–8</sup> To obtain further information on the hydrogen bonding of PVA, we are trying to apply similar CP/MAS  $^{13}\text{C}$  NMR analyses to different PVA solutions in the frozen state. In this paper, we report the first results indicating the formation of intramolecular hydrogen bonding in the frozen solution state and its great dependencies on solvents and tacticities of PVA, as observed by frozen-state NMR spectroscopy. These results further support the previous assignment for the formation of intramolecular hydrogen bonding.

Atactic PVA (A-PVA)<sup>2,3</sup> and highly isotactic PVA (HI-PVA),<sup>9,10</sup> which were provided by Kuraray Co., were used after purification through complete saponification. The triad tacticities determined by solution-state  $^1\text{H}$  NMR spectroscopy and the viscosity-average degrees of polymerization (DP) are as follows:  $mm = 0.23$ ,  $mr = 0.50$ ,  $rr = 0.27$ , and  $\text{DP} = 1700$  for A-PVA and  $mm = 0.79$ ,  $mr = 0.19$ ,  $rr = 0.02$ , and  $\text{DP} = 9100$  for HI-PVA. Each PVA was dissolved in deionized water or dimethyl sulfoxide (DMSO) at  $120^\circ\text{C}$  in a glass tube sealed under an atmosphere of argon. Each solution thus obtained was packed into a cylindrical MAS rotor with an O-ring seal<sup>2</sup> and frozen in the rotating state at a rate of about 1 kHz in a CP/MAS probe by decreasing the temperature up to  $-50^\circ\text{C}$ . CP/MAS  $^{13}\text{C}$  NMR spectra of these frozen samples were measured at  $-50^\circ\text{C}$  on a JEOL JNM-GSX200 spectrometer operating at a static magnetic field of 4.7 T.  $^1\text{H}$  and  $^{13}\text{C}$  radio-frequency fields,  $\gamma B_1/2\pi$ , were 69.4 kHz, the MAS rate being 3.5 kHz. The CP contact time was set to 1 ms, and the delay time after the acquisition of free induction decays was 5 s throughout this work.

Figure 1 shows CP/MAS  $^{13}\text{C}$  NMR spectra of frozen A-PVA aqueous solutions measured at  $-50^\circ\text{C}$ . For reference, the CP/MAS  $^{13}\text{C}$  spectrum for A-PVA films prepared from the 10 wt % aqueous solution is also shown in this figure. Here, the contributions from the materials used for the MAS rotor and the probe were removed by subtracting the spectrum obtained by the blank measurement from the corresponding spectra. Interestingly, two lines assigned to lines II and III appear at almost the same chemical shifts as those for

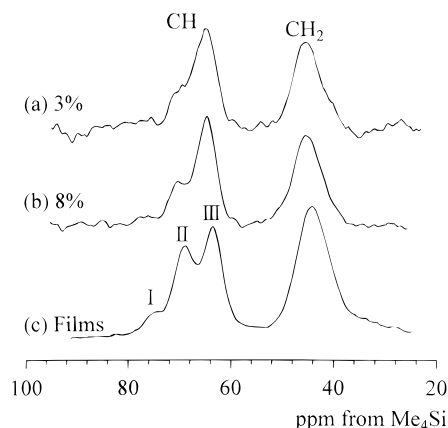


**Figure 1.** CP/MAS  $^{13}\text{C}$  NMR spectra of frozen A-PVA aqueous solutions with different concentrations, measured at  $-50^\circ\text{C}$ .

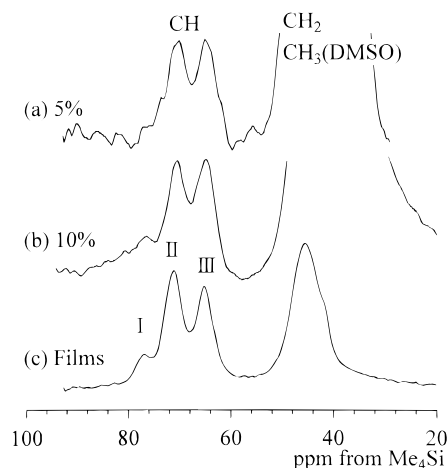


**Figure 2.** CP/MAS  $^{13}\text{C}$  NMR spectra of frozen A-PVA/DMSO solutions with different concentrations, measured at  $-50^\circ\text{C}$ . The  $\text{CH}_2$  resonance line is superposed on the huge contribution from the  $\text{CH}_3$  carbon of DMSO.

PVA films even in the frozen solution state. Moreover, the relative intensity of the splitting lines, which is almost independent of the PVA concentration, is greatly different from that for the films: Line II is markedly decreased in intensity compared to the case of the films, and the resonance line ascribed to line I is hardly detectable.

In contrast to the results in the frozen aqueous solution, line II is greatly increased in intensity in the frozen DMSO solution, as shown in Figure 2. Moreover, line I is clearly observed similarly to the case of the films. These observations really support our previous assignment<sup>1–3</sup> that lines I, II, and III are ascribed to the central CH carbons in triad sequences associated with the formation of two, one, and no intramolecular hydrogen bond(s), because such changes in intensity for the same atactic sample should not be interpreted by the substitution effects.<sup>4,5</sup> According to this assignment, only a small amount of the intramolecular hydrogen bonds may be formed in an isolated state in the frozen aqueous solution. In contrast, some intramolecular hydrogen bonds will be continuously formed along the PVA chain as a result of the increase in the total fraction of intramolecular hydrogen bonds. It should also be noted here that the concentration of PVA seems not to appreciably affect the formation of hydrogen bonds in both solutions at least in this range of concentration. In addition, almost the same clear aqueous or DMSO

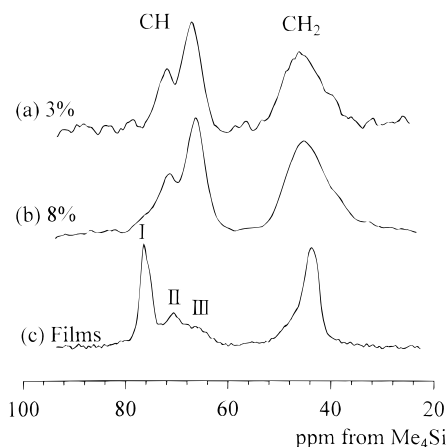


**Figure 3.** CP/MAS  $^{13}\text{C}$  NMR spectra of frozen HI-PVA aqueous solutions with different concentrations, measured at  $-50^\circ\text{C}$ .

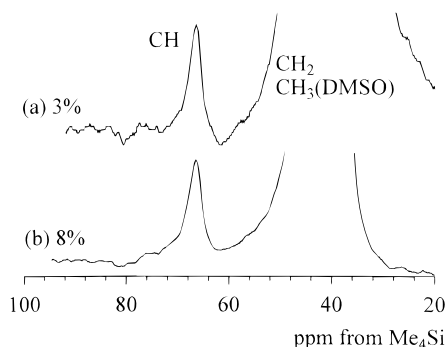


**Figure 4.** CP/MAS  $^{13}\text{C}$  NMR spectra of frozen HI-PVA/DMSO solutions with different concentrations, measured at  $-50^\circ\text{C}$ . The  $\text{CH}_2$  resonance line is superposed on the huge contribution from the  $\text{CH}_3$  carbon of DMSO.

solutions were obtained at room temperature after the NMR measurements, indicating no apparent formation of gels.

Figure 3 shows the corresponding CP/MAS  $^{13}\text{C}$  NMR spectra of frozen HI-PVA aqueous solutions. Here, the spectrum for HI-PVA films prepared from the 10 wt % aqueous solution is also shown for reference. Almost the same spectra are obtained in the frozen state as the case of A-PVA, although the relative intensities of lines I, II, and III are greatly different between A-PVA films and HI-PVA films. Moreover, only a single resonance line assigned to line III is observed in the frozen DMSO solutions, as shown in Figure 4. These results suggest that the probability of the formation of the intramolecular hydrogen bonds may greatly depend on solvents as well as tacticities. No formation of gels was also confirmed in both solutions at room temperature after the NMR measurements.

In the crystalline state, we have already derived equations<sup>3,6</sup> to estimate the probabilities  $p_a$  and  $p_e (=1 - p_a)$  for the formation of the intramolecular and intermolecular hydrogen bonds for planar zigzag chains from the relative intensities of lines I, II, and III, using crystal structure models proposed by Sakurada *et al.*<sup>11</sup> and Bunn.<sup>12</sup> Here, it is assumed that there is no deshielding effect of the formation of the intermolecular hydrogen bonding on the chemical shift of the CH carbon, because the oxygen–oxygen distance is as long as over 0.27 nm in the intermolecular hydrogen bonds compared to 0.25 nm for the intramolecular hydrogen bond in PVA.<sup>1–3,11,12</sup> In the noncrystalline state, however, the existence of the *gauche* conformation should be considered and the intramolecular hydrogen bonds are also allowed to form in the *r* sequences when the *gauche* conformation is appropriately introduced. For example, the same type of intramolecular hydrogen bonds can be formed in the *mr* sequence as in the *mm* sequence, when the chain conformations are *tttg<sup>-</sup>* for *mr* and *ttt* for *mm*, respectively. Here, the conformations *trans* (*t*) and *gauche* (*g*) should be defined for the triad sequence  $\text{CH}(\text{OH})\text{--CH}_2\text{--CH}(\text{OH})\text{--CH}_2\text{--CH}(\text{OH})$ . Furthermore, the so-called  $\gamma$ -*gauche* effect<sup>13</sup> should be correctly elucidated in this treatment. As for the intermolecular hydrogen bonding including that with solvent molecules, no deshielding effect may also appear in the frozen solution state, because the oxygen–oxygen distance should be more than about 0.27 nm in most cases. Those problems pointed out here will be critically discussed in the near future, together with a more detailed experimental examination of the effects of the cooling process for PVA solutions.

## References and Notes

- (1) Terao, T.; Maeda, S.; Saika, A. *Macromolecules* **1983**, *15*, 1535.
- (2) Horii, F.; Hu, S.; Ito, T.; Odani, H.; Kitamaru, R.; Matsuzawa, S.; Yamamura, K. *Polymer* **1992**, *33*, 2299.
- (3) Hu, S.; Tsuji, M.; Horii, F. *Polymer* **1994**, *35*, 2516.
- (4) Ketels, H.; de Haan, J.; Aerdts, A.; van der Velden, G. *Polymer* **1990**, *31*, 1419.
- (5) Imashiro, F.; Obara, S. *Macromolecules* **1995**, *28*, 2840.
- (6) Hu, S.; Horii, F.; Odani, H. *Bull. Inst. Chem. Res., Kyoto Univ.* **1991**, *69*, 165.
- (7) Hu, S.; Horii, F.; Odani, H.; Narukawa, H.; Akiyama, A.; Kajitani, K. *Kobunshi Ronbunshu* **1992**, *49*, 361.
- (8) Masuda, K.; Hu, S.; Kaji, H.; Horii, F. *Polym. Prepr. Jpn.* **1996**, *45*, 3260.
- (9) Ohgi, H.; Sato, T. *Macromolecules* **1993**, *26*, 559.
- (10) Horii, F.; Hu, S.; Deguchi, K.; Sugisawa, H.; Ohgi, H.; Sato, T. *Macromolecules* **1996**, *29*, 3330.
- (11) Sakurada, I.; Fuchino, K.; Okada, N. *Bull. Inst. Chem. Res., Kyoto Univ.* **1950**, *23*, 78.
- (12) Bunn, C. W. *Nature* **1948**, *161*, 929.
- (13) Tonelli, A. E. *NMR Spectroscopy and Polymer Microstructure: The Conformational Connection*; VCH: New York, 1989.

MA961708U